HHS Public Access

Author manuscript

J Micromech Microeng. Author manuscript; available in PMC 2019 October 04.

Published in final edited form as:

J Micromech Microeng. 2017 ; 27(1): .

Mixing high-viscosity fluids via acoustically driven bubbles

Sinem Orbay[1], **Adem Ozcelik**[2], **James Lata**[2], **Murat Kaynak**[2], **Mengxi Wu**[2], **Tony Jun Huang**[1,2]

Tony Jun Huang: junhuang@psu.edu

[1]Department of Biomedical Engineering, The Pennsylvania State University, University park, PA 16802, USA.

[2]Department of Engineering Science and Mechanics, The Pennsylvania State University, University park, PA 16802, USA.

Abstract

We present an acoustofluidic micromixer which can perform rapid and homogeneous mixing of highly viscous fluids in the presence of an acoustic field. In this device, two high-viscosity polyethylene glycol (PEG) solutions were co-injected into a three-inlet PDMS microchannel with the center inlet containing a constant stream of nitrogen flow which forms bubbles in the device. When these bubbles were excited by an acoustic field generated via a piezoelectric transducer, the two solutions mixed homogenously due to the combination of acoustic streaming, droplet ejection, and bubble eruption effects. The mixing efficiency of this acoustofluidic device was evaluated using PEG-700 solutions which are ~106 times more viscous than deionized (DI) water. Our results indicate homogenous mixing of the PEG-700 solutions with a ~0.93 mixing index. The acoustofluidic micromixer is compact, inexpensive, easy to operate, and has the capacity to mix highly viscous fluids within 50 milliseconds.

Keywords

Micromixing; high-viscosity fluid; acoustofluidics; polyethylene glycol (PEG)

1. Introduction

Microfluidic technology provides a plethora of unique benefits to the scientific and medical communities including small sample volume, low reagent consumption, low cost, high sensitivity, and high precision [1–4]. However, working at a low Reynolds number (Re) presents significant challenges for mixing highly viscous fluids in a microfluidic device [5–7]. Numerous microfluidic diagnosis and analysis platforms require handling of such high-viscosity fluids in applications including biochemical reactors [8–11], biological sample preparation [12–14], and bioanalysis [15–17]. For example, sputum, which is an important source for disease detection [14,18], needs to be liquefied and mixed with biological reagents prior to analysis [13]. Furthermore, many biological or chemical processes, such as syntheses and reactions, require a rapid mixing of reagents to yield a homogeneous mixture before the reaction has completed [19–24].

Regardless of the liquid's viscosity, mixing within a microfluidic device is not a trivial matter, as diffusive mixing is slow, requiring more than 100 seconds to mix fluids within a simple 100 μm wide microchannel [25]. When flow is introduced into a continuous flow device, fluids flow in low Re laminar flow regimes with small diffusive transport through the liquid-liquid interface. To address the challenge of fluid mixing, two major categories of microfluidic mixers have been reported: active and passive mixers. Passive micromixers, such as diffusion driven [26,27] and chaotic advection based [28–31], utilize the flow velocity and channel geometry to redirect and split the flow in the microfluidic channel. Whereas active micromixers, such as thermal [32], optical [33], magnetic [34,35], electrokinetic [36–38], and acoustic-based [39–45], use external forces to break laminar flow and induce fluid mixing. An acoustic based micromixer was reported to mix high-viscosity fluids via bubble generation and acoustic streaming, but the reported mixing time (2–4 s) was prohibitively long for fast occurring chemical reactions [45]. Li *et al.* demonstrated passive mixing of a moderate viscosity (~35 mPa s) fluid, but homogeneous mixing occurred only at relatively high Re (~ 73.27) [6]. Our group recently developed a high-viscosity micromixer using acoustofluidic bubble inception and oscillations from the microchannel sidewalls, and achieved homogenous mixing of polyethylene glycol diacrylate (PEGDA) and deionized (DI) water solutions with a viscosity of 48 mPa s within 100 milliseconds [5]. In this method, bubble initiation and growth required a relatively high driving voltage (160 V_{PP}), and was not well controlled due to random emergence of bubble initiation sites. Overall viscosity of the mixed fluids was limited because bubble nucleation and initiation requirements were not adequate to mix higher-viscosity liquids. Due to the range of issues with current strategies, a new method of high-viscosity micromixing is necessary for rapid and consistently homogeneous results.

Acoustic bubbles have been widely used in various microfluidic platforms for applications including fluid manipulation [46], mixing [47], cell stimulation [48], chemical gradient generation [49] and particle manipulation [50–52]. In this work, we developed an acoustofluidic device for mixing high-viscosity fluid via acoustically driven bubbles in a microchannel. This micromixer utilizes strong bubble oscillations, which include steady microstreaming and jetting effects [53], to continuously mix high-viscosity fluids. It is shown here to achieve rapid and effective mixing of clear and fluorescein dyed PEG solutions at very low Re (~ 0.01). The acoustofluidic micromixer is simple in design and operation, and can be used in many lab-on-a-chip applications which involve high-viscosity fluids under low Reynolds numbers.

2. Method

A single-layer, polydimethylsiloxane (PDMS) microfluidic channel with width, depth, and length of 250 μm, 100 μm, and 1.2 mm was first fabricated using standard photolithography and replica molding techniques. In short, a 4-inch silicon wafer was pretreated with hexamethyldisilazane (HMDS) and patterned with a positive photoresist (Megaposit SPR955, Microchem, USA). Then, a silicon master mold was fabricated using deep reactive ion etching (DRIE). After surface treatment of the silicon mold with chlorotrimethylsilane vapor (75-77-4, Alfa Aesar, USA), a 10:1 ratio of PDMS resin and curing agent (Sylgard 184, Dow-Corning, USA) was cured and demolded from the master mold. A biopsy punch

(Harris Uni-Core 0.75 mm, USA) was used to open inlets and outlets of the PDMS microchannels. After plasma treatment of the PDMS device and a glass slide (48404–454, VWR, USA), strong bonding was achieved via overnight baking at 65 °C. A piezoelectric transducer (90–4050, APC, USA) was bonded next to the PDMS device using a thin layer of epoxy (Part#G14250, Devcon, USA). The piezoelectric transducer was driven using a radio frequency (RF) signal generator (AFG3011, Tektronix, USA) and an RF power amplifier (25A250A, Amplifier Research, USA) at 60–100 V_{pp} (peak to peak) and 30–40 kHz. Operation frequency was obtained by sweeping the frequency and observing the maximum mixing performance of the bubbles. Polyethylene tubes were inserted into the inlets and outlets of the PDMS device.

Fluids to be mixed were injected into the channel using a computer-controlled syringe pump (neMESYS, Germany) at a flow rate of 5 μl/min for each fluid. Bubbles were generated in the center inlet of the device using a connected nitrogen tank with an inline pressure regulator which was adjusted for optimum bubble generation (1–10 psi). For the collection of bubble-free mixed fluid, a bubble-filter was designed in front of the second outlet of the device (see Supplementary figure 1). An inverted optical microscope (TE-2000U, Nikon, Japan) was used for capturing still images and movies. Fluorescence imaging utilized a mercury lamp (Intense Light C-HGFI, Nikon, Japan) and blue excitation filter (B-2E/C, Nikon, Japan). As for the fluorescence emitting fluid, 10 ml PEG-700 (455008, Sigma-Aldrich, USA) was mixed with 0.01 mg fluorescein powder (F7250, Sigma-Aldrich, USA), and injected into one of the side inlets. To demonstrate bubble generation and its effect on fluid mixing, PEG-700 was mixed with food dye at a ratio of 20:1 (v/v), and injected into the channel with clear PEG-700.

3. Results and Discussion

In our acoustofluidic micromixing device (figure 1(a)), the mixing behavior is based on the steady acoustic streaming and jetting effects [53] between the series of bubbles within the microchannel as demonstrated in figure 1(b). These bubbles are generated by nitrogen gas which is infused from the center inlet of the device. Bubble generation in similar three-inlet devices have been widely studied and found mostly dependent on the device geometry and flow rates of the fluids in the side inlets [54,55]. In our experiments, we use highly viscous PEG-700 solutions as the fluids in the side inlets at 5 μl/min flow rates. By adjusting the nitrogen pressure in the center inlet from 1 to 10 psi, we obtain nitrogen bubble packages along the channel with desired frequency and size. For example, figures 2(a)–(d) shows bubble generation at 4 psi nitrogen pressure and 10 μl/min total flow rate. When the acoustic field is OFF, PEG-700 and PEG-700 + food dye solutions flow without any significant mixing after the bubble generation (figure 2(d)), which suggest that the bubble generation itself does not cause any observable mixing behavior (see Supplementary Movie 1). Furthermore, when only the acoustic field is applied without any bubbles present in the microchannel, the mixing is minimal at 100 V_{pp} (see Supplementary Movie 2). On the other hand, when the acoustic field is turned ON in the presence of the bubbles, three phenomena that contribute to high-viscosity fluid mixing occur in the microchannel due to the acoustically excited bubbles.

Firstly, once the acoustic field is turned ON, bubbles act as the focusing agents of the acoustic energy and start oscillating depending on the excitation frequency of the acoustic field [53,56,57]. These oscillations at the gas-liquid interface cause a harmonic forcing on the fluid at this interface. The response of the fluid to this force is not harmonic due to the viscous dissipation of energy in the channel; instead it results in a net fluid flow known as acoustic streaming [56]. Strong acoustic streaming in the PEG-700 solutions contributes to the mass transfer and ultimately the fluid mixing (figure 3 and Supplementary Movie 3). Acoustic streaming due to trapped bubbles was also demonstrated to generate fluid mixing [49,58], but excitation of the trapped bubbles was kept to a small voltage (<20 V_{PP}) which is not enough to generate significant streaming in high-viscosity fluids. The reason for using small excitation voltages in trapped bubble systems is to prevent bubble growth and unstable jetting events, which could cause device blocking or bubble escape, and render the device unusable. We found that high-amplitude bubble oscillations are necessary in our highly viscous system.

Secondly, at higher oscillation amplitudes, gas-liquid interfaces start pulling and pushing fluids which contribute to fluid mixing through liquid transfer across the bubble (Supplementary Movie 4). As seen from figures 3(e)–(g), when the gas-liquid interface oscillates vigorously, a small amount of liquid forms a ligament which later becomes disconnected and forms a droplet inside the bubble. These droplets move at high speeds and join to the liquid at the other end of the bubble pocket. These bubble-mediated “droplet ejection” events cause fluid mixing due to fluid transfer from one side to the other and associated fluid flows. This droplet generation and ejection is an interesting finding that can be further investigated for microfluidic static-flow droplet generation or liquid-liquid phase separation.

Thirdly, smaller bubbles and bubble clusters erupt from the larger bubble pockets (figures 3(c) and (d)), thus generating steady acoustic streaming and jetting [59,60] across the channel width which in turn induces fluid mixing (Supplementary Movie 5). A collapsing bubble generates both jetting and counter rotating vortices that are estimated to rotate at 10,000 rev/s [61]. Bremond ετ. αλ. also reported on bubble-bubble interactions and resulted jetting flows with the conclusion that bubble cluster cavitations generate jetting flows directed towards the center of the cluster [62]. In another study, velocity of the jetting flow due to a collapsing bubble was estimated to be around 25 m/s [63]. We believe that high-viscosity fluid mixing occurs as a result of the combination of acoustic streaming, droplet ejection, and bubble cluster eruption.

In order to demonstrate the mixing performance of our acoustofluidic devices, we used different concentrations of PEG-700 solutions. For each concentration, the PEG and PEG + fluorescein solutions are injected from the two liquid inlets of the PDMS device. In figure 4(a), PEG-700 (95.9 mPa s) with and without fluorescein dye are injected into the upper (white) and lower (black) inlets, respectively. In the absence of the acoustic field, there is no significant fluid mixing between the two flows. When the transducer is turned ON, the two fluids are mixed within 50 milliseconds (figure 4(b)). Grayscale profiles along the dotted line in figures 4(a) and (b) show homogenous mixing along the channel width (figure 4(c)). We also examined the mixing profiles of the two fluids at different channel heights (see

Supplementary figure 2). At the bottom, middle, and top of the channel, mixing profiles shows very similar intensity plots suggesting uniform mixing along the height of the channel. We also quantitatively evaluate the mixing performance for each PEG-700 concentration using the following equation [6]:

$$M = 1 - \frac{\sqrt{1/n \sum (I_i - I_m)^2}}{I_m} \quad (1)$$

where M is the mixing index, n is the total number of points, I_i is the intensity of each point, and I_m is the average intensity. For unmixed flows M becomes 0, and for completely mixed fluids M becomes 1. A mixing index value of 0.9 or higher indicates homogenous mixing [6,64]. We characterized the mixing index of seven different solutions with viscosity values varying from 0.899 mPa s for DI water to 95.9 mPa s for PEG-700 (figure 5). Even for the highest-viscosity PEG-700 solution, we observe a mixing index around 0.93 which suggest efficient and rapid mixing of two highly viscous fluids. Mixing index values for the mixed fluids at different heights of the channel are also found to be similar to each other. The Re of our high-viscosity fluid system is calculated to be ~0.01 which is significantly lower than prior high-viscosity micromixers [6,45].

4. Conclusions

In summary, we present an acoustofluidic mixer that can mix two highly viscous fluids (95.9 mPa s), which are ~106 times more viscous than DI water (0.899 mPa s), within 50 milliseconds. For this task, we used a three-inlet PDMS microchannel where high-viscosity fluids are injected from the side inlets and nitrogen bubbles are introduced in the center inlet. In the presence of an acoustic field, seven different solutions with viscosities ranging from 0.899 mPa s to 95.9 mPa s were mixed and the resulted mixed fluids were quantitatively analyzed using the mixing index value (M). When two 100% PEG-700 (95.9 mPa.s) solutions are mixed, the mixing efficiency is calculated to be ~0.93. Overall, we demonstrate high-viscosity fluid mixing in a low Reynolds number system (~0.01) within 50 milliseconds. Our acoustofluidic mixing device has many desirable properties such as simple fabrication, low cost, on-demand and easy operation. These properties make our acoustofluidic device ideal for integration into other lab-on-a-chip systems. In future studies, we will evaluate the effects of our acoustofluidic mixer on cell viability and cell membrane structure. The strong streaming and jetting flows that are confined in our acoustofluidic device could be useful to achieve intracellular delivery of nanoparticles and plasmid DNA in a straightforward manner. The presented acoustofluidic micromixer can potentially be used in various on-chip applications including sample preparation, diagnosis, biochemical reactions, and chemical synthesis.

Supplementary Material

Refer to Web version on PubMed Central for supplementary material.

Acknowledgement

We acknowledge support from National Institutes of Health (R01 GM112048 and R33 EB019785), National Science Foundation (CBET-1438126 and IDBR-1455658), and the Center for Nanoscale Science, a National Science Foundation (NSF) Materials Research Science and Engineering Center supported under DMR-1420620. Sinem Orbay, Adem Ozcelik, and Murat Kaynak acknowledge the support from Turkey's Ministry of National Education.

Reference

[1]. Mei Q, Xia Z, Xu F, Soper S a and Fan ZH 2008 Fabrication of microfluidic reactors and mixing studies for luciferase detection. Anal. Chem 80 6045–50 [PubMed: 18593194]

[2]. Mao X and Huang TJ 2012 Microfluidic diagnostics for the developing world. Lab Chip 12 1412–6 [PubMed: 22406768]

[3]. Ashtiani AO and Jiang H 2013 Thermally actuated tunable liquid microlens with sub-second response time Appl. Phys. Lett 103 111101

[4]. Lee H, Xu L, Koh D, Nyayapathi N and Oh K 2014 Various On-Chip Sensors with Microfluidics for Biological Applications Sensors 14 17008–36 [PubMed: 25222033]

[5]. Ozcelik A, Ahmed D, Xie Y, Nama N, Qu Z, Nawaz AA and Huang TJ 2014 An acoustofluidic micromixer via bubble inception and cavitation from microchannel sidewalls. Anal. Chem 86 5083–8 [PubMed: 24754496]

[6]. Li Y, Xu Y, Feng X and Liu B 2012 A rapid microfluidic mixer for high-viscosity fluids to track ultrafast early folding kinetics of G-quadruplex under molecular crowding conditions. Anal. Chem 84 9025–32 [PubMed: 23020167]

[7]. Agarwal AK, Sridharamurthy SS, Beebe DJ and Hongrui Jiang 2005 Programmable autonomous micromixers and micropumps J. Microelectromechanical Syst 14 1409–21

[8]. Pollack L, Tate MW, Darnton NC, Knight JB, Gruner SM, Eaton W aAustin RH 1999 Compactness of the denatured state of a fast-folding protein measured by submillisecond small-angle x-ray scattering. Proc. Natl. Acad. Sci. U. S. A 96 10115–7 [PubMed: 10468571]

[9]. Park HY, Qiu X, Rhoades E, Korlach J, Kwok LW, Zipfel WR, Webb WW and Pollack L 2006 Achieving uniform mixing in a microfluidic device: hydrodynamic focusing prior to mixing. Anal. Chem 78 4465–73 [PubMed: 16808455]

[10]. Xie Y, Ahmed D, Lapsley MI, Lin SS, Nawaz AA, Wang L and Huang TJ 2012 Single-shot characterization of enzymatic reaction constants Km and kcat by an acoustic-driven, bubble-based fast micromixer. Anal. Chem 84 7495–501 [PubMed: 22880882]

[11]. Schabas G, Yusuf H, Moffitt MG and Sinton D 2008 Controlled self-assembly of quantum dots and block copolymers in a microfluidic device. Langmuir 24 637–43 [PubMed: 18184020]

[12]. Basu AS and Gianchandani YB 2008 Virtual microfluidic traps, filters, channels and pumps using Marangoni flows J. Micromechanics Microengineering 18 115031

[13]. Huang P-H, Ren L, Nama N, Li S, Li P, Yao X, Cuento RA, Wei C-H, Chen Y, Xie Y, Nawaz AA, Alevy YG, Holtzman MJ, McCoy JP, Levine SJ and Huang TJ 2015 An acoustofluidic sputum liquefier Lab Chip 15 3125–31 [PubMed: 26082346]

[14]. Feather EA and Russell G 1970 Sputum viscosity in cystic fibrosis of the pancreas and other pulmonary diseases Br. J. Dis. Chest 64 192–200 [PubMed: 5533003]

[15]. Lillehoj PB, Wei F and Ho C-M 2010 A self-pumping lab-on-a-chip for rapid detection of botulinum toxin Lab Chip 10 2265 [PubMed: 20596556]

[16]. Lillehoj PB, Huang M-C, Truong N and Ho C-M 2013 Rapid electrochemical detection on a mobile phone Lab Chip 13 2950 [PubMed: 23689554]

[17]. Khandurina J and Guttman A 2002 Bioanalysis in microfluidic devices J. Chromatogr. A 943 159–83 [PubMed: 11833638]

[18]. Xie Y, Todd NW, Liu Z, Zhan M, Fang H, Peng H, Alattar M, Deepak J, Stass SA and Jiang F 2010 Altered miRNA expression in sputum for diagnosis of non-small cell lung cancer. Lung Cancer 67 170–6 [PubMed: 19446359]

[19]. Lee W-B, Weng C-H, Cheng F-Y, Yeh C-S, Lei H-Y and Lee G-B 2009 Biomedical microdevices synthesis of iron oxide nanoparticles using a microfluidic system. Biomed. Microdevices

[20]. Chan EM, Marcus M a, Fakra S, ElNaggar M, Mathies R a and Alivisatos a P 2007 Millisecond kinetics of nanocrystal cation exchange using microfluidic X-ray absorption spectroscopy. J. Phys. Chem. A

[21]. Rondeau E and Cooper-White JJ 2008 Biopolymer microparticle and nanoparticle formation within a microfluidic device. Langmuir

[22]. Nightingale AM and de Mello JC 2010 Microscale synthesis of quantum dots J. Mater. Chem

[23]. Karnik R, Gu F, Basto P, Cannizzaro C, Dean L, Kyei-Manu W, Langer R and Farokhzad OC 2008 Microfluidic platform for controlled synthesis of polymeric nanoparticles. Nano Lett. 8 2906–12 [PubMed: 18656990]

[24]. Lee KH, Shin SJ, Kim C-B, Kim JK, Cho YW, Chung BG and Lee S-H 2010 Microfluidic synthesis of pure chitosan microfibers for bio-artificial liver chip. Lab Chip 10 1328 [PubMed: 20445889]

[25]. Mao X, Juluri BK, Lapsley MI, Stratton ZS and Huang TJ 2009 Milliseconds microfluidic chaotic bubble mixer Microfluid. Nanofluidics 8 139–44

[26]. Suh YK and Kang S 2010 A Review on Mixing in Microfluidics Micromachines 1 82–111

[27]. Kakuta M, Jayawickrama DA, Wolters AM, Manz A and Sweedler JV. 2003 Micromixer-Based Time-Resolved NMR: Applications to Ubiquitin Protein Conformation Anal. Chem 75 956–60 [PubMed: 12622391]

[28]. Therriault D, White SR and Lewis JA 2003 Chaotic mixing in three-dimensional microvascular networks fabricated by direct-write assembly. Nat. Mater 2 265–71 [PubMed: 12690401]

[29]. Stroock AD, Dertinger SKW, Ajdari A, Mezic I, Stone HA and Whitesides GM 2002 Chaotic mixer for microchannels. Science 295 647–51 [PubMed: 11809963]

[30]. Frommelt T, Kostur M, Wenzel-Schafer M, Talkner P, Hanggi P, Wixforth A, Wenzel-Schäfer M, Talkner P, Hänggi P and Wixforth A 2008 Microfluidic Mixing via Acoustically Driven Chaotic Advection Phys. Rev. Lett 100 034502 [PubMed: 18232985]

[31]. Aref H. 1984; Stirring by chaotic advection. J. Fluid Mech. 143:1.

[32]. Tsai J and Lin L 2002 Active microfluidic mixer and gas bubble filter driven by thermal bubble micropump Sensors Actuators A Phys. 97–98 665–71

[33]. Hellman AN, Rau KR, Yoon HH, Bae S, Palmer JF, Phillips KS, Allbritton NL and Venugopalan V 2007 Laser-induced mixing in microfluidic channels. Anal. Chem 79 4484–92 [PubMed: 17508715]

[34]. Ryu KS, Shaikh K, Goluch E, Fan Z and Liu C 2004 Micro magnetic stir-bar mixer integrated with parylene microfluidic channels. Lab Chip 4 608–13 [PubMed: 15570373]

[35]. Zhu G-P and Nguyen N-T 2012 Rapid magnetofluidic mixing in a uniform magnetic field. Lab Chip 12 4772–80 [PubMed: 22990170]

[36]. Chang C-C and Yang R-J 2007 Electrokinetic mixing in microfluidic systems Microfluid. Nanofluidics 3 501–25

[37]. Sigurdson M, Wang D and Meinhart CD 2005 Electrothermal stirring for heterogeneous immunoassays. Lab Chip 5 1366–73 [PubMed: 16286967]

[38]. Lee C-Y, Lee G-B, Lin J-L, Huang F-C and Liao C-S 2005 Integrated microfluidic systems for cell lysis, mixing/pumping and DNA amplification J. Micromechanics Microengineering 15 1215–23

[39]. Phan H Van, Coşkun MB, Şeşen M, Pandraud G, Neild A and Alan T 2015 Vibrating membrane with discontinuities for rapid and efficient microfluidic mixing Lab Chip 15 4206–16 [PubMed: 26381355]

[40]. Sesen M, Alan T and Neild A 2015 Microfluidic plug steering using surface acoustic waves Lab Chip 15 3030–8 [PubMed: 26079216]

[41]. Ahmed D, Chan CY, Lin S-CS, Muddana HS, Nama N, Benkovic SJ, Jun Huang T, Huang TJ, Jun Huang T, Huang TJ, Jun Huang T and Huang TJ 2013 Tunable, pulsatile chemical gradient generation via acoustically driven oscillating bubbles. Lab Chip 13 328–31 [PubMed: 23254861]

[42]. Wang S, Huang X and Yang C 2012 Microfluidic Bubble Generation by Acoustic Field for Mixing Enhancement J. Heat Transfer 134 051014

[43]. Ahmed D, Mao X, Juluri BK and Huang TJ 2009 A fast microfluidic mixer based on acoustically driven sidewall-trapped microbubbles Microfluid. Nanofluidics 7 727–31

[44]. Tseng W-K, Lin J-L, Sung W-C, Chen S-H and Lee G-B 2006 Active micro-mixers using surface acoustic waves on Y-cut 128° LiNbO 3 J. Micromechanics Microengineering 16 539–48

[45]. Wang S, Huang X and Yang C 2011 Mixing enhancement for high viscous fluids in a microfluidic chamber. Lab Chip 11 2081–7 [PubMed: 21547315]

[46]. Hashmi A, Heiman G, Yu G, Lewis M, Kwon H-J and Xu J 2012 Oscillating bubbles in teardrop cavities for microflow control Microfluid. Nanofluidics 14 591–6

[47]. Wang C, Rallabandi B and Hilgenfeldt S 2013 Frequency dependence and frequency control of microbubble streaming flows Phys. Fluids 25 022002

[48]. Chen D, Sun Y, Gudur MSR, Hsiao Y-S, Wu Z, Fu J and Deng CX 2015 Two-Bubble Acoustic Tweezing Cytometry for Biomechanical Probing and Stimulation of Cells Biophys. J 108 32–42 [PubMed: 25564850]

[49]. Ahmed D, Muddana HS, Lu M, French JB, Ozcelik A, Fang Y, Butler PJ, Benkovic SJ, Manz A and Huang TJ 2014 Acoustofluidic Chemical Waveform Generator and Switch Anal. Chem 86 11803–10 [PubMed: 25405550]

[50]. Tan JN, Ling WYL and Neild A 2013 Selective Liquid Droplet Transfer Using Injected Bubbles Appl. Phys. Express 6 077301

[51]. Phan HV, Şeşen M, Alan T and Neild A 2014 Single line particle focusing using a vibrating bubble Appl. Phys. Lett 105 193507

[52]. Wang C, Jalikop SV and Hilgenfeldt S 2012 Efficient manipulation of microparticles in bubble streaming flows. Biomicrofluidics

[53]. Hashmi A, Yu G, Reilly-Collette M, Heiman G and Xu J 2012 Oscillating bubbles: a versatile tool for lab on a chip applications. Lab Chip 12 4216–27 [PubMed: 22864283]

[54]. Dollet B, van Hoeve W, Raven J-P, Marmottant P and Versluis M 2008 Role of the Channel Geometry on the Bubble Pinch-Off in Flow-Focusing Devices Phys. Rev. Lett 100 034504 [PubMed: 18232987]

[55]. Xu L, Lee H, Panchapakesan R and Oh KW 2012 Fusion and sorting of two parallel trains of droplets using a railroad-like channel network and guiding tracks Lab Chip 12 3936 [PubMed: 22814673]

[56]. Sadhal SS 2012 Acoustofluidics 16: acoustics streaming near liquid-gas interfaces: drops and bubbles. Lab Chip

[57]. Liu RH, Yang J, Pindera MZ, Athavale M and Grodzinski P 2002 Bubble-induced acoustic micromixing. Lab Chip 2 151–7 [PubMed: 15100826]

[58]. Ahmed D, Mao X, Shi J, Juluri BK and Huang TJ 2009 A millisecond micromixer via single-bubble-based acoustic streaming. Lab Chip 9 2738–41 [PubMed: 19704991]

[59]. Bremond N, Arora M, Ohl C-D and Lohse D 2005 Cavitation on surfaces J. Phys. Condens. Matter 17 S3603–8

[60]. Bremond N, Arora M, Ohl C-D and Lohse D 2005 Cavitating bubbles on patterned surfaces Phys. Fluids 17 091111

[61]. Zwaan E, Le Gac S, Tsuji K and Ohl C-D 2007 Controlled Cavitation in Microfluidic Systems Phys. Rev. Lett 98 254501 [PubMed: 17678027]

[62]. Bremond N, Arora M, Ohl C-D and Lohse D 2006 Controlled Multibubble Surface Cavitation Phys. Rev. Lett 96 224501 [PubMed: 16803310]

[63]. Versluis M, Schmitz B, von der Heydt A and Lohse D 2000 How Snapping Shrimp Snap: Through Cavitating Bubbles Science 289 2114–7 [PubMed: 11000111]

[64]. Hashmi A and Xu J 2014 On the Quantification of Mixing in Microfluidics J. Lab. Autom 19 488–91 [PubMed: 24963095]

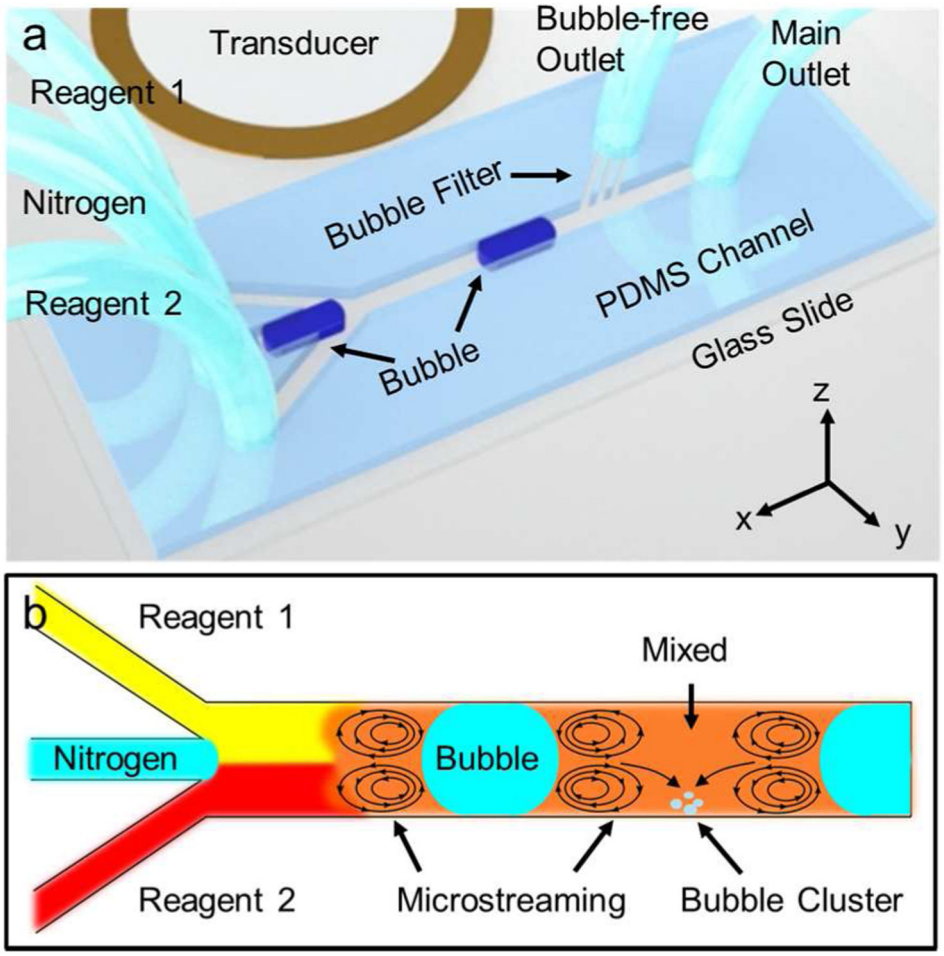

Figure 1.

(a) A schematic shows the acoustofluidic mixing device (not to scale). A PDMS-based microfluidic channel and a piezoelectric transducer are assembled on a glass slide. High-viscosity fluids and nitrogen bubbles are injected from the side and center inlets, respectively. (b) Working principle of the acoustofluidic mixing device is depicted as a cartoon illustration.

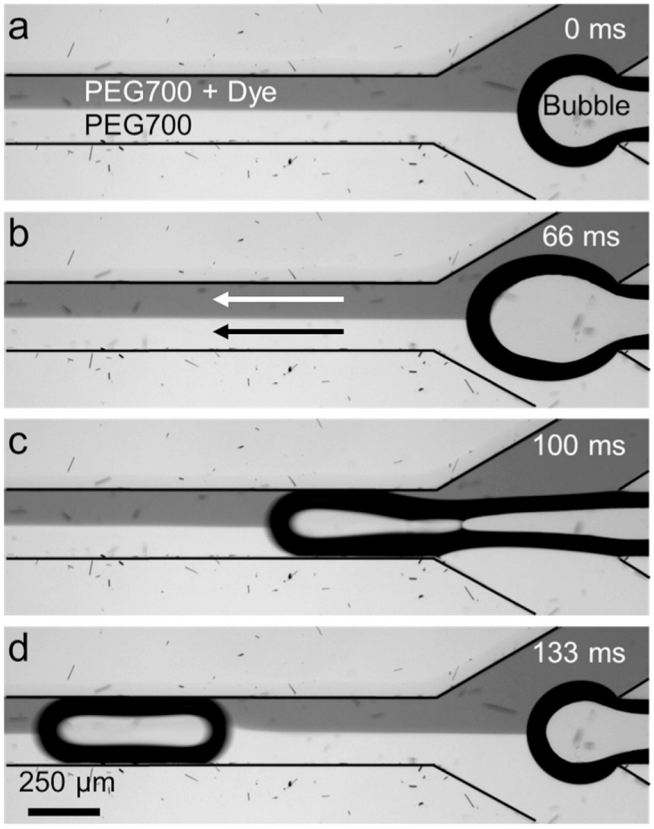

Figure 2.

Image sequence showing bubble generation in the PDMS microfluidic channel. PEG-700 solution with and without food dye was injected from the top and bottom inlets at 5 μl/min, and nitrogen bubbles were injected from the center inlet at ~4 psi. The acoustic field is off.

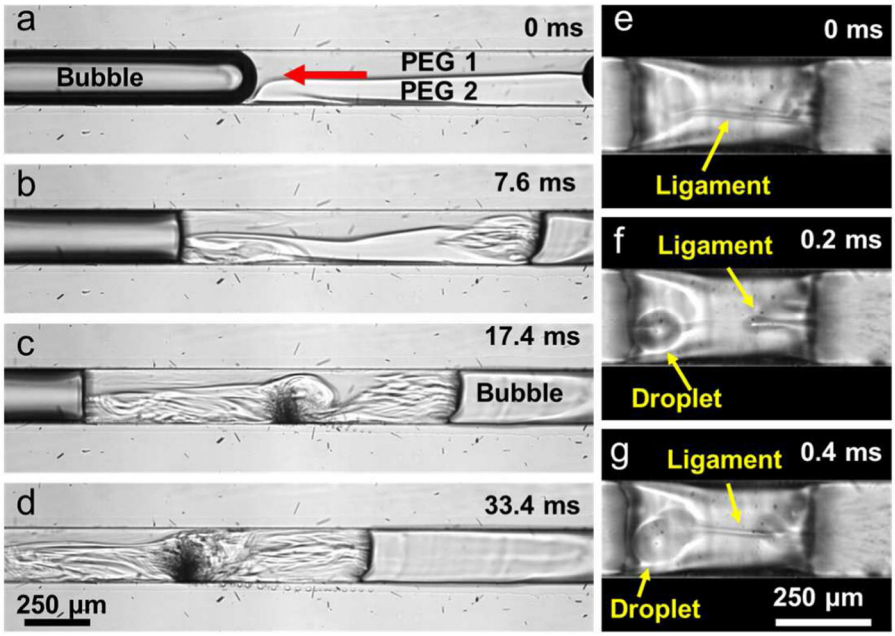

Figure 3.

(a)–(d) Bubble streaming flows were visualized between two bubble pockets using fluorescein dyed (PEG 1) and clear (PEG 2) PEG-700 solutions at 80 V_{pp}. As a result of partial bubble disintegration, smaller bubbles and bubble clusters are formed between two bubble pockets and contribute to the mixing. (e)–(g) Liquid ligament formation and droplet ejection occurs due to strong air-liquid interface oscillations.

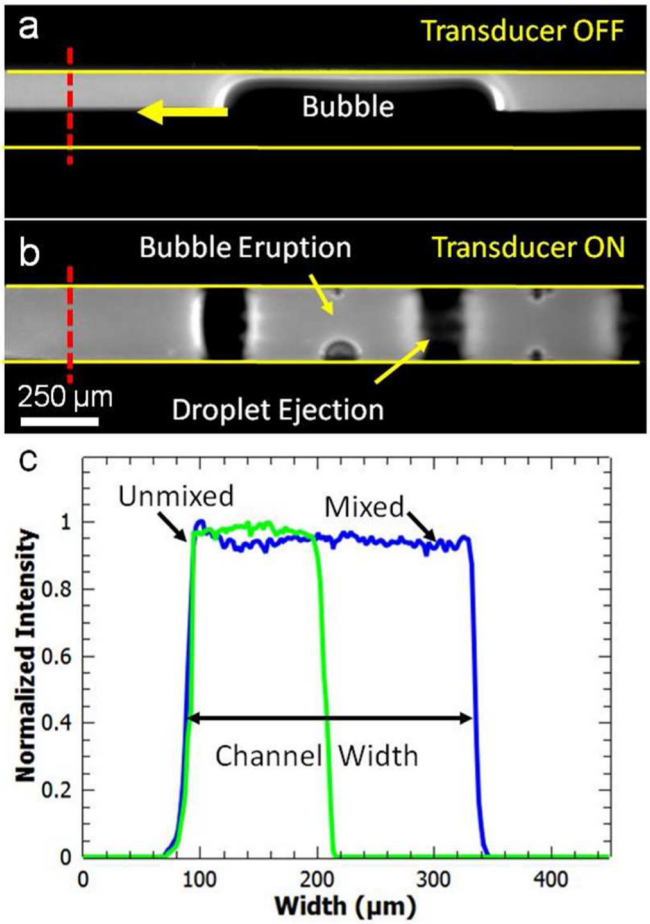

Figure 4.

(a) PEG-700 with and without fluorescein dye, and bubbles are smoothly flowing along the microchannel in the absence of an acoustic field, displaying no significant mixing due to bubble generation. (b) When the piezoelectric transducer is turned ON (~100 V_{PP}), 100 % PEG-700 with and without fluorescein dye are mixed in 50 milliseconds. (c) Grayscale intensity plot (normalized to 1) along the dotted lines in (a) and (b) shows homogenous mixing after the acoustic transducer is turned ON.

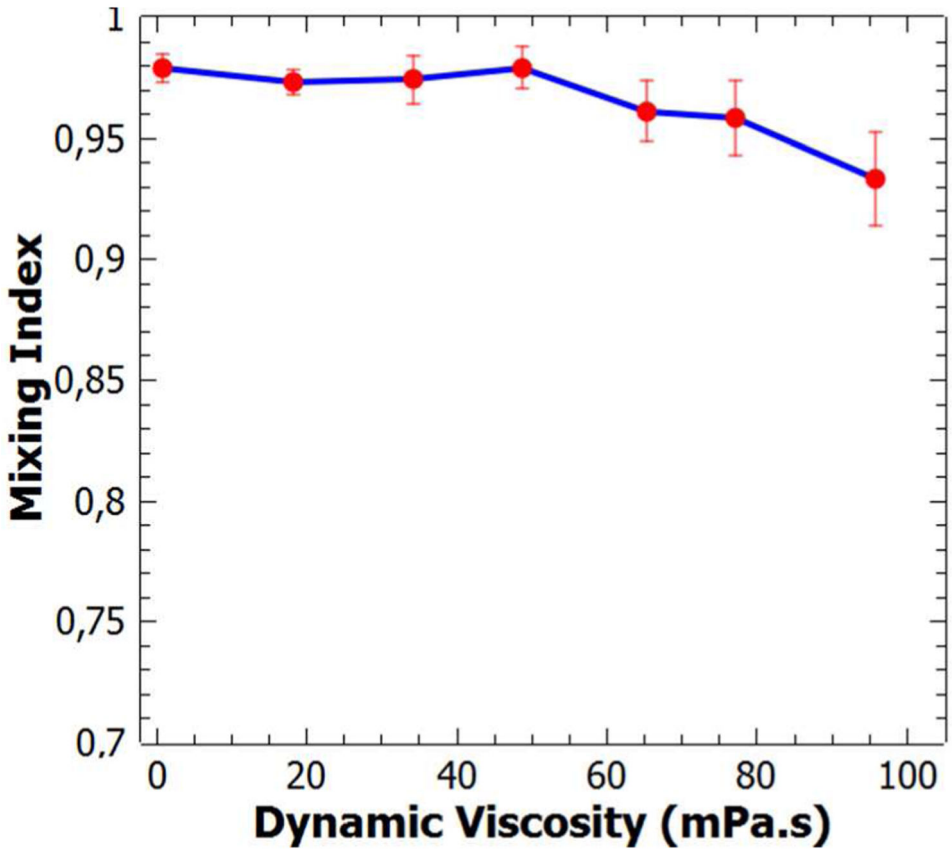

Figure 5.

Calculated mixing index values for DI water and PEG-700 solutions with a range of viscosities. Mixing index value for 100 % PEG-700 solution is found to be above 0.9. The error bars represent the standard deviation of the repeated experiments (n≥5).